DOI: 10.1002/chem.201103641

Pentacoordinate Ni^{II} Complexes: Preparation, Magnetic Measurements, and Ab Initio Calculations of the Magnetic Anisotropy Terms

Jean-Pierre Costes,*[a, b] Rémi Maurice ,*[c, d, e] and Laure Vendier[a, b]

Abstract: Two novel mononuclear five-coordinate nickel complexes with distorted square-pyramidal geometries are presented. They result from association of a tridentate "half-unit" ligand and 6,6′-dimethyl-2,2′-bipyridine according to a stepwise process that highlights the advantage of coordination chemistry in isolating an unstable tridentate ligand by nickel chelation. Their zero-field splittings (ZFS) were studied by means of magnetic data and state-of-the-art ab initio calculations. Good agreement between the experimental and theoretical axial *D* parameters confirms that large single-ion nickel anisotropies are accessible. The synthetic process can also yield dinuclear nickel complexes in which the nickel ions are hexacoordinate. This possibility is facilitated by the presence of phenoxo oxygen atoms in the tridentate ligand that can introduce a bridge between the two nickel ions. Two different double bridges are characterized, with the bridging oxygen atoms coming from each nickel ion or from the same nickel ion. This coordination change introduces a difference in the antiferromagnetic interaction parameter *J*. Although the magnetic data confirm the presence of single-ion anisotropies in these complexes, these terms cannot be determined in a straightforward way from experiment due to the mismatch between the principal axes of the local anisotropies and the presence of intersite anisotropies.

Keywords: ab initio calculations · magnetic properties · nickel · N,O ligands · tridentate ligands

Introduction

Magnetic anisotropy, which is an important property of magnetic molecules and materials, can be accessed by diverse theoretical and experimental techniques, depending on the system. In the case of mononuclear transition metal complexes, various experimental approaches can be used, such as frequency-domain magnetic resonance spectroscopy (if the spin quantum number of the ground state is an integer) and high-field high-frequency electron paramagnetic resonance.[1] From a theoretical point of view, the anisotropic magnetic parameters can be accessed by methods based on DFT[2–7] or wave-function theory (WFT).[8] We recently confirmed that WFT-based ab initio calculations can give valuable information in the case of nickel complexes containing only one active metal ion,[9] in agreement with previous work.[10] The same approach has been also successfully applied to high-spin Co^{II} and Mn^{III} mononuclear complexes,[10–11] and could be further applied to any d^n mononuclear complex for which the spin Hamiltonian approach is relevant.

The anisotropy of binuclear complexes can be determined in the same way, as shown by previous studies dealing with homobinuclear copper complexes.[12–13] However, homobinuclear nickel complexes were found more problematic, since a rigorous description of the multispin model requires the introduction of a biquadratic anisotropic exchange tensor.[14] Such modeling prohibits any extraction from the effective Hamiltonian theory, since too many parameters are introduced in the model. Due to this shortcoming, alternatives such as the giant-spin model, which considers only the effective anisotropy of the ground spin state (in the case of ferromagnetic coupling), or a block-spin model that considers the anisotropy of all the different spin states in a block diagonal model matrix can be envisaged. In the strong-exchange regime, one can consider that spin mixing (i.e., the effective coupling between the components of the different spin states that can originate from local anisotropies or symmetric and antisymmetric anisotropic interactions) is negligible,

[a] Dr. J.-P. Costes, Dr. L. Vendier
CNRS, LCC (Laboratoire de Chimie de Coordination)
205, route de Narbonne, 31077 Toulouse (France)
E-mail: jean-pierre.costes@lcc-toulouse.fr

[b] Dr. J.-P. Costes, Dr. L. Vendier
Université de Toulouse, UPS, INPT, LCC, 31077 Toulouse (France)

[c] Dr. R. Maurice
Laboratoire de Chimie et de Physique Quantique
IRSAMC/UMR5626, Université de Toulouse III
118 route de Narbonne, 31062 Toulouse Cedex 4 (France)
E-mail: remi.maurice@gmail.com

[d] Dr. R. Maurice
Departament de Química Física i Inorganica
Universitat Rovira i Virgili
Marcel.lí Domingo s/n, 43007 Tarragona (Spain)

[e] Dr. R. Maurice
Zernike Institute for Advanced Materials, University of Groningen
Nijenborgh 4; 9747AG Groningen (The Netherlands)

Supporting information for this article is available on the WWW under http://dx.doi.org/10.1002/chem.201103641 It contains figures showing the field dependence of the magnetization for complexes **2**, **3**, and **8** at 2 K and the temperature dependence of $\chi_M T$ for **8** from 300 to 2 K.

and hence that such models fully account for all important effective interactions. However, in the weak-exchange limit, spin mixing must be introduced into the model.[15,16] For centrosymmetric complexes, spin mixing only affects the singlet and some components of the quintet spin state and can be theoretically estimated in a rigorous and straightforward way by using the effective Hamiltonian theory.[17] If antisymmetric interactions are allowed by symmetry, all of the different spin states can strongly mix due to symmetric and antisymmetric interactions, so that the giant-spin and block-spin pictures become no longer relevant. A practical and rigorous model of such a situation has not yet been achieved, so that any standard reliable extraction from experiment is prohibited.

Synthesis of complexes with large single-ion anisotropies is of primary importance to further design polynuclear complexes with slow relaxation of the magnetization at low temperatures, that is, single-molecule magnets (SMMs). Nickel coordination chemistry[18] is mainly dominated by octahedral or square-planar coordination. However, six-coordinate and four-coordinate complexes usually have small anisotropy parameters and, even worse, low-spin ground states, respectively. Nonstandard coordination numbers, such as pentacoordinate complexes, can then be used to obtain interesting complexes with significant anisotropies.[1] Such complexes can ideally show regular square-pyramidal (SPY) or trigonal-bipyramidal (TBP) geometries or span distorted geometries between these two ideal forms. It is expected that complexes of distorted geometries should have large zero-field splitting (ZFS) parameters, with an axial D parameter that can be either positive (close to SPY geometry) or negative (close to TBP geometry). In the TBP geometry, first-order spin–orbit coupling between the components of the two orbitally degenerate configurations would be observed, prohibiting use of the spin Hamiltonian approach. It is then of first importance to find accessible preparative pathways leading to new pentacoordinate complexes, preferably with geometries close to SPY or intermediate between SPY and TBP.

Five-coordinate complexes have been mainly prepared by use of similar or different monodentate ligands or by using combinations of bidentate or tridentate chelating ligands with monodentate ligands, while combinations of a tridentate and a bidentate ligand have been much less considered.[19] In the past, we have described synthetic pathways that could furnish several tridentate ligands, thanks to the template effect of copper ions,[20] but this preparative pathway appears to be limited to copper chemistry and does not work in the presence of nickel ions. Later, we described a synthetic pathway leading to a nickel complex involving a tridentate ligand resulting from reaction of hydroxyacetophenone with 2-methyl-1,2-diaminopropane.[21] Unfortunately, this process is limited to the latter diamine, which shows steric crowding of one amino group. To extend it to more interesting diamines such as 1,2-diaminopropane, we report on a process that allows preparation of diamagnetic nickel complexes in which a tridentate and a monodentate ligand are linked to the nickel ion in square-planar coordination. Further reaction with bipyridine or a substituted bipyridine should yield the expected pentacoordinate Ni complexes. However, we will show that the combination of a tridentate and a bidentate ligands in the nickel coordination sphere does not necessarily give a pentacoordinate nickel complex. Experimental magnetic studies and ab initio calculations on two mononuclear pentacoordinate complexes confirm the presence of large axial zero-field splitting D terms. Magnetic measurements on the two binuclear complexes will be presented, and the difficulties encountered in interpreting them commented on.

Experimental Section

The ligand 2-[(1*E*)-*N*-(2-amino-2-methylpropyl)ethanimidoyl]phenol (HL^1) was prepared as previously described.[21] $Ni(OAc)_2{\cdot}4H_2O$, $NaClO_4$, hydroxyacetophenone, isopropylamine, 2-methyl-1,2-diaminopropane, 1,2-diaminopropane, (*S*)-1,2-diaminopropane dihydrochloride, 2,2′-bipyridine, and 6,6′-dimethyl-2,2′-bipyridine (Aldrich) were used as purchased. High-grade solvents (methanol, ethanol) and distilled water were used for the preparation of the different complexes.

Caution! Because of their explosive character, perchlorate salts should be handled with care and in very small amounts.

$[L^1Ni(iPrNH_2)]ClO_4$ (1): A solution of hydroxyacetophenone (1.36 g, 10 mmol) and 2-methyl-1,2-diaminopropane (0.88 g, 10 mmol) in methanol (80 mL) was stirred and heated to 50 °C for 20 min. Then NaOH (0.42 g, 10 mmol) was added, followed 10 min later by addition of $Ni(Ac)_2{\cdot}4H_2O$ (2.50 g, 10 mmol) and isopropylamine (0.59 g, 10 mmol). The mixture was stirred and heated for 30 min. The solution was reduced to half-volume and the precipitate that appeared was filtered off and dried. Yield: 2.3 g (54 %). Elemental analysis (%) calcd for $C_{15}H_{26}ClN_3NiO_5$ (422.5): C 42.6, H 6.2, N 9.9; found: C 42.3, H 6.0, N 9.7; IR: $\tilde{\nu}$ = 3310m, 3271m, 3235m, 3156m, 2976m, 1599s, 1574s, 1526m, 1467w, 1439m, 1395w, 1377w, 1357m, 1340w, 1260w, 1230m, 1158m, 1101s, 1080s, 1047s, 1021w, 931w, 913w, 873w, 823w, 758s, 738m, 621s cm^{-1}.

$[L^1Ni(2,2'\text{-bipy})]_2(ClO_4)_2$ (2): A solution of $[L^1Ni(iPrNH_2)]ClO_4$ (0.09 g, 0.21 mmol) and of 2,2′-bipyridine (0.033 g, 0.21 mmol) in methanol (2 mL) was stirred at room temperature for 10 min. The green precipitate that appeared was filtered off and washed with cold methanol and diethyl ether. Diffusion of diethyl ether into a methanol solution of the crude product yielded crystals suitable for X-ray analysis. Yield: 0.05 g (45 %). Elemental analysis (%) calcd for $C_{22}H_{25}ClN_4NiO_5$ (519.6): C 50.9, H 4.9, N 10.8; found: C 50.3, H 4.9, N 10.5; IR: $\tilde{\nu}$ = 3324m, 3271w, 3059w, 2939w, 1613m, 1605m, 1591m, 1549m, 1471m, 1439s, 1372w, 1300m, 1255w, 1235w, 1157w, 1082s, 1059s, 1019s, 944w, 905w, 847m, 765m, 737m, 621m cm^{-1}.

$[L^1Ni(6,6'\text{-diMe-}2,2'\text{-bipy})]ClO_4$ (3): A solution of $[L^1Ni(iPrNH_2)]ClO_4$ (0.10 g, 0.23 mmol) and of 6,6′-dimethyl-2,2′-bipyridine (0.044 g, 0.23 mmol) in methanol (3 mL) was heated to 50 °C for 10 min. Cooling the stirred solution gave a maroon precipitate, which was filtered off and washed with cold methanol and diethyl ether. Diffusion of diethyl ether to an acetone solution of the crude product yielded crystals suitable for X-ray analysis. Yield: 0.045 g (35 %). Elemental analysis (%) calcd for $C_{24}H_{29}ClN_4NiO_5$ (547.7): C 52.6, H 5.3, N 10.2; found: C 52.3, H 5.1, N 9.9; IR: $\tilde{\nu}$ = 3288m, 3255m, 3179m, 2972w, 1601s, 1580s, 1533m, 1464m, 1435m, 1395w, 1379w, 1325m, 1259w, 1221m, 1167w, 1108s, 1092s, 1070s, 1031m, 1018m, 948w, 922w, 914w, 853w, 788s, 761s, 621s cm^{-1}.

$[L^2Ni(OAc)]$ (4): An ethanol solution (40 mL) of hydroxyacetophenone (1.36 g, 10 mmol) was added dropwise at room temperature to a stirred ethanol solution of 1,2-diaminopropane (0.74 g, 10 mmol). Stirring was continued for 4 h and followed by addition of $Ni(OAc)_2{\cdot}4H_2O$ (2.50 g, 10 mmol). The mixture was heated to 50 °C for 20 min and then cooled to

room temperature under stirring, leaving an orange precipitate (1.9 g), which was isolated by filtration and dried. 0.45 g of this precipitate was poured into dichloromethane (60 mL) and stirred for 30 min. Filtration yielded an orange precipitate, which was dried by washing with diethyl ether (10 mL). Yield: 0.30 g (41%). Elemental analysis (%) calcd for $C_{13}H_{18}N_2NiO_3$ (309.0): C 50.5, H 5.9, N 9.1; found: C 50.5, H 5.9, N 9.0; IR: $\tilde{\nu}$ = 3221m, 3077w, 2966w, 1596s, 1578s, 1527m, 1445m, 1381s, 1350m, 1326m, 1298w, 1243m, 1219w, 1164w, 1150m, 1136m, 1052w, 1017w, 918w, 869w, 783w, 748m, 740m, 684w, 659w cm^{-1}.

$[L^2Ni(Ph(Me)CH(R)NH_2)]ClO_4$ (5): Part of the crude orange precipitate obtained above (0.5 g) was added to water, stirred for 30 min, and filtered off. Addition of (*R*)-1-phenylethylamine (0.15 g, 1,2 mmol) and sodium perchlorate (0.2 g, 16 mmol) to the stirred aqueous solution induced precipitation of an orange-red product, which was filtered off one hour later and dried. Recrystallization from methanol yielded crystals suitable for X-ray analysis. Yield: 0.32 g (42%). Elemental analysis (%) calcd for $C_{19}H_{26}ClN_3NiO_5$ (470.6): C 48.5, H 5.6, N 8.9; found: C 48.3, H 5.4, N 8.7; IR: $\tilde{\nu}$ = 3318w, 3292m, 3264w, 3237m, 3152w, 2974w, 1600m, 1578s, 1527m, 1454w, 1441m, 1345m, 1318w, 1285w, 1243m, 1198w, 1146m, 1104s, 1085m, 1051s, 1010w, 930w, 915w, 875w, 848w, 756s, 719w, 700m, 621m cm^{-1}.

$[L^2Ni(2,2'\text{-bipy})]ClO_4$ (6): A solution of $[L^2Ni(Ph(Me)CH(R)NH_2)]ClO_4$ (0.12 g, 0.29 mmol) and of 2,2′-bipyridine (0.046 g, 0.29 mmol) in methanol (2 mL) was stirred at room temperature for 10 min. The green solution that formed was filtered. Diffusion of diethyl ether into a methanol solution of the crude product yielded crystals suitable for X-ray analysis. Yield: 0.08 g (54%). Elemental analysis (%) calcd for $C_{21}H_{23}ClN_4NiO_5$ (505.6): C 49.9, H 4.6, N 11.1. Found: C 49.6, H 4.5, N 10.9; IR: $\tilde{\nu}$ = 3343w, 3339w, 3291w, 3287w, 2965w, 1608m, 1602m, 1590m, 1547m, 1472m, 1437s, 1374w, 1310m, 1296m, 1252w, 1236m, 1170w, 1106m, 1077s, 1056s, 1023m, 938w, 853m, 846m, 761s, 736m, 652w, 620m cm^{-1}.

$[L^2(S)Ni(Ph(Me)CH(R)NH_2)]ClO_4$ (7): (*S*)-1,2-Diaminopropane dihydrochloride (1.0 g, 6.8 mmol) and NaOH (0.54 g, 13.6 mmol) were dissolved in water (7 mL) with stirring. Ethanol was added and the resulting solution was filtered 15 min later. Hydroxyacetophenone (0.92 g, 6.8 mmol) was added to the filtrate and the resulting solution was stirred at room temperature overnight. After addition of $Ni(OAc)_2{\cdot}4H_2O$ (1.7 g, 6.8 mmol) and stirring at room temperature for 2 h, the mixture was filtered to eliminate the precipitate (0.23 g). Addition of (*R*)-1-phenylethylamine (0.5 g, 4.1 mmol) and sodium perchlorate (0.6 g, 4.9 mmol) to the stirred filtrate induced precipitation of an orange-red product, which was filtered off one hour later and dried. Recrystallization from methanol yielded crystals suitable for X-ray analysis. Yield: 1.2 g (37%). Elemental analysis (%) calcd for $C_{19}H_{26}ClN_3NiO_5$ (470.6): C 48.5, H 5.6, N 8.9; found: C 48.4, H 5.5, N 8.7; IR: $\tilde{\nu}$ = 3275s, 3227m, 3148m, 2969w, 1596m, 1585s, 1533m, 1456w, 1436m, 1382w, 1334m, 1293w, 1243m, 1227w, 1187w, 1134s, 1066s, 1046s, 931w, 919w, 871w, 853w, 752s, 700m, 621s cm^{-1}.

$[L^2(S)Ni(6,6'\text{-diMe-}2,2'\text{-bipy})]ClO_4{\cdot}MeOH$ (8): A solution of $[L^2(S)Ni(PhMe)CH(R)NH_2]ClO_4$ (0.10 g, 0.21 mmol) and of 6,6′-dimethyl-2,2′-bipyridine (0.044 g, 0.23 mmol) in methanol (3 mL) was heated to 50 °C for 20 min. The cooled solution, which was kept undisturbed, yielded crystals suitable for X-ray analysis two days later. Yield: 0.03 g (25%). Elemental analysis (%) calcd for $C_{24}H_{31}ClN_4NiO_6$ (565.7): C 51.0, H 5.2, N 9.9; found: C 50.8, H 5.1, N 9.7; IR: $\tilde{\nu}$ = 3294m, 3258m, 3176m, 2971w, 2911w, 1600s, 1575s, 1532m, 1454m, 1439m, 1396w, 1374w, 1335m, 1259w, 1231m, 1167w, 1148w, 1091s, 1070s, 1033m, 930w, 912w, 854w, 787s, 761s, 621s cm^{-1}.

Physical measurements: Elemental analyses were carried out at the Laboratoire de Chimie de Coordination Microanalytical Laboratory in Toulouse, France, for C, H, and N. IR spectra were recorded on a Perkin-Elmer Spectrum 100 FTIR spectrophotometer in ATR mode. Magnetic data were obtained with a Quantum Design MPMS SQUID susceptometer. Magnetic susceptibility measurements were performed in the 2–300 K temperature range in a 0.1 T applied magnetic field, and diamagnetic corrections were applied by using Pascal's constants.[22] Isothermal magnetization measurements were performed up to 5 T at 2 K. The magnetic susceptibilities were computed by exact calculations of the energy levels associated to the spin Hamiltonian through diagonalization of the full matrix with a general program for axial and rhombic symmetries,[23] and the magnetizations with the MAGPACK program package.[24] Least-squares fittings were accomplished with an adapted version of the function-minimization program MINUIT.[25]

Crystallographic data collection and structure determinations: Crystals were kept in the mother liquor until they were dipped into oil. The chosen crystals were mounted on a Mitegen micromount and quickly cooled to 180 K. The selected crystals of **2** (yellow, 0.3×0.18×0.06 mm), **3** (brown, 0.25×0.15×0.03 mm), **5** (orange, 0.3×0.18×0.08 mm), **6** (yellow, 0.2×0.15×0.06 mm), **7** (orange, 0.23×0.08×0.05 mm), and **8** (green, 0.25×0.20×0.12 mm) were mounted on an Oxford Diffraction Xcalibur diffractometer equipped with graphite-monochromated $Mo_{K\alpha}$ radiation (λ = 0.71073 Å) and an Oxford Instrument Cooler Device. Data were collected at 180 K. The final unit cell parameters were obtained by least-squares refinement. The structures were solved by direct methods using SIR92,[26] and refined by means of least-squares procedures on F^2 with the program SHELXL97[27] included in the software package WinGX version 1.63.[28] The atomic scattering factors were taken from the *International Tables for X-Ray Crystallography*.[29] All non-hydrogen atoms were anisotropically refined, and in the last cycles of refinement a weighting scheme was used, where weights were calculated from the following formula: $w = 1/[\sigma^2(F_o^2) + (aP)^2 + bP]$ where $P = (F_o^2 + 2F_c^2)/3$. Drawings of molecules were generated with the program ORTEP32 with 30% probability displacement ellipsoids for non-hydrogen atoms.[30]

CCDC-854361 (**2**), CCDC-854362 (**3**), CCDC-854363 (**5**), CCDC-854364 (**6**), CCDC-854365 (**7**), and CCDC-854366 (**8**) contain the supplementary crystallographic data for this paper. These data can be obtained free of charge from The Cambridge Crystallographic Data Centre via www.ccdc.cam.ac.uk/data_request/cif

Calculations: All calculations are performed by using the ORCA program, v. 2.8.[31] A two-step WFT based approach was chosen. A set of nonrelativistic states was first computed at the complete active space self-consistent field (CASSCF) level. Scalar relativistic effects were neglected in the computation of the spin-orbit free states, and state-averaged molecular orbitals (MOs) were used to compute the whole d^8 manifold of the mononuclear Ni^{II} complexes. Correlated energies were obtained at the *n*-electron valence state second-order perturbation theory (NEVPT2) level.[32–34] The relativistic effects responsible for the zero-field splitting, that is, both spin–spin coupling (SSC) and spin–orbit coupling (SOC) were included a posteriori. The SOC Hamiltonian is approximated in a mean-field way,[35,36] and the Breit–Pauli SSC Hamiltonian is used. A state-interaction (SI) matrix between the spin–orbit components of the different spin–orbit free states was built and diagonalized to account for the effect of the SSC and SOC on the ZFS parameters, which were extracted by using the effective Hamiltonian theory.[37,38] In the principal axes frame, the axial *D* and rhombic *E* parameters and the magnetic anisotropy axes are defined such as Equation (1)

$$|D| = \left| D_{ZZ} - \frac{1}{2}(D_{XX} + D_{YY}) \right| > 3E = \frac{3}{2}(D_{XX} - D_{YY}) > 0 \quad (1)$$

The Def2 basis sets and the corresponding auxiliary basis sets[39] were used for all atoms. The following contraction schemes were taken: 6s5p4d2f1g for Ni atoms, 5s3p2d1f for O and N atoms, 3s2p1d for C atoms, and 2s for H atoms. The complexes were taken in their experimental structures.

Results

We have previously shown that with help of the copper template effect, it was possible to isolate copper complexes of half-units resulting from single condensation of salicylaldehyde with only one amino group of a 1,2- or 1,3-diamine.[20] Unfortunately, this reaction does not work when copper ions are replaced by nickel ions. We got around the problem

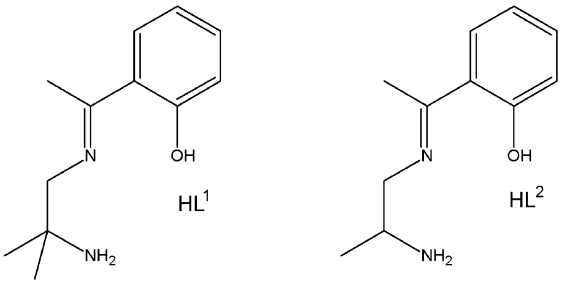

Scheme 1. 2-[(1*E*)-*N*-(2-Amino-2-methylpropyl)ethanimidoyl]phenol (HL^1) and 2-[(1*E*)-*N*-(2-aminopropyl)ethanimidoyl]phenol (HL^2).

by use of 2-hydroxyacetophenone and 1,2-diamino-2-methylpropane (Scheme 1). Indeed the ketone group can only react with the unhindered NH_2 group of 1,2-diamino-2-methylpropane, leading to a HL^1 half-unit 2-[(1*E*)-*N*-(2-amino-2-methylpropyl)ethanimidoyl]phenol that can thereafter chelate a nickel ion[21] to give a square-planar diamagnetic nickel complex with three equatorial positions occupied by the chelating half-unit and the fourth by an N ligand (pyridine or isopropylamine), as in the present work. This experimental process is limited, so we decided to extend it to more reactive diamines, such as 1,2-diaminopropane. NMR studies clearly show that the reaction of 2-hydroxyacetophenone and 1,2-diaminopropane in dichloromethane in 1/1 ratio gives a mixture of the expected HL^2 half-unit along with the Schiff base H_2L^3 corresponding to the reaction of the two amine groups with 2-hydroxyacetophenone (Scheme 2). So we repeated the reaction in ethanol at room

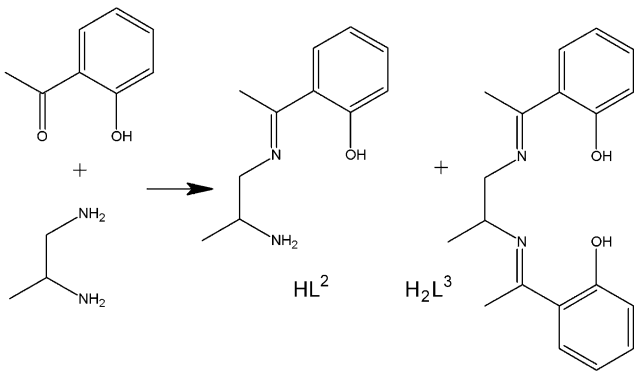

Scheme 2.

temperature, followed by addition of solid nickel acetate and short heating at 50 °C. The solid precipitate that appeared was isolated by filtration from the cold solution. At this stage, the isolated solid can be treated in two different ways. Partial dissolution in dichloromethane and filtration of the resulting solution left a solid precipitate, which was again washed with dichloromethane and dried. Analytical data confirmed its formulation as [L^2Ni(OAc)] (**4**) (L^2 = 2-[(1*E*)-*N*-(2-aminopropyl)ethanimidoyl]phenolate). From the dichloromethane solution, it is possible to recover complex [L^3Ni]. The other possibility consists of adding water to the isolated solid with stirring and filtering the resulting solution. Addition of an amine to the filtrate induces a color change of the aqueous solution from colorless to red-orange, followed by precipitation of [L^2Ni{Ph(Me)CH(*R*)NH_2}]ClO_4 (**5**), which was isolated by filtration and dried. This experimental process allows the L^3Ni complex to be isolated as a solid. This last pathway is the preferred one, for we succeeded in obtaining crystals of complex **5**, which was not the case with complex **4**. Until now, the unavailability of quality crystals for complex **4** impeded its structure determination. Further reaction of the diamagnetic and cationic nickel complexes **1** and **5** with 2,2′-bipyridine or 6,6′-dimethyl-2,2′-bipyridine yielded complexes **2**, **3**, and **6**, in which the corresponding bipyridine has entered the nickel coordination sphere after removal of the monodentate amine ligand. This process was also realized with the (*S*)-1,2-diaminopropane enantiomer instead of the racemic 1,2-diaminopropane, yielding the orange complex **7**, which reacts with 6,6′-dimethyl-2,2′-bipyridine to give green complex **8**.

Structural analyses: Crystallographic data of complexes **2**, **3**, **5**, **6**, **7**, and **8** are collected in Table 1. The 2-[(1*E*)-*N*-(2-amino-2-methylpropyl)ethanimidoyl]phenol ligand HL^1 was previously characterized,[21] and we did not try to determine the structure of complex **1**, which is used as starting material for the preparation of the pentacoordinate complexes. On the contrary, structures of the complexes involving the 2-[(1*E*)-*N*-(2-aminopropyl)ethanimidoyl]phenol ligand HL^2 in its racemic (**5**) or enantiomerically pure form (**7**) were solved (Figures 1 and 2, respectively). Both compounds crystallize in the noncentrosymmetric space group $P2_1$. The nickel ions display the expected square-planar coordination through two nitrogen atoms and one oxygen atom of the chelating tridentate ligand, and the fourth equatorial position is occupied by the nitrogen atom of (*R*)-1-phenylethylamine. The use of the monodentate amine in its enantiomerically pure form is responsible for the observation of

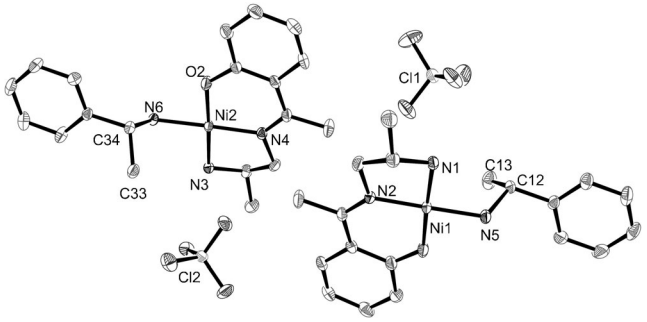

Figure 1. Plot of complex **5** with ellipsoids drawn at 30 % probability and partial atom numbering. Hydrogen atoms have been omitted for clarity. Selected bond lengths [Å] and angles [°]: Ni1–O1 1.800(2), Ni1–N1 1.885(3), Ni1–N2 1.891(3), Ni1–N5 1.929(3), Ni2–O2 1.802(2), Ni2–N3 1.891(3), Ni2–N4 1.863(3), Ni2–N6 1.929(3); O1-Ni1-N2 95.24(11), O1-Ni1-N5 84.78(11), N1-Ni1-N2 87.34(11), N1-Ni1-N5 92.68(11), O1-Ni1-N1 176.69(13), N2-Ni1-N5 178.80(14), O2-Ni2-N4 95.76(11), O2-Ni2-N6 84.38(11), N3-Ni2-N4 87.10(12), N3-Ni2-N6 92.85(11), O2-Ni2-N3 175.76(14), N4-Ni2-N6-178.33(14).

Table 1. Crystallographic data for complexes **2**, **3**, **5**, **6**, **7**, and **8**.

	2	**3**	**5**	**6**	**7**	**8**
formula	$C_{44}H_{50}Cl_2N_8Ni_2O_{10}$	$C_{24}H_{29}ClN_4NiO_5$	$C_{19}H_{26}ClN_3NiO_5$	$C_{42}H_{46}Cl_2N_8Ni_2O_{10}$	$C_{19}H_{26}ClN_3NiO_5$	$C_{24}H_{31}ClN_4NiO_6$
M_r	1039.24	547.67	470.57	1011.15	470.59	565.69
space group	$P\bar{1}$	$C2/c$	$P2_1$	$C2/c$	$P2_1$	$P1$
a [Å]	12.7651(4)	28.2396(16)	11.4746(4)	9.8774(3)	5.769(5)	8.1971(3)
b [Å]	12.8456(4)	14.1278(7)	7.9722(3)	23.2185(6)	10.924(5)	11.7028(4)
c [Å]	15.2769(5)	13.0817(9)	23.2133(8)	19.4974(5)	16.610(5)	13.5417(5)
α [°]	81.649(3)	90	90	90	90	89.472(3)
β [°]	76.802(3)	106.695(7)	90.121(3)	98.303(3)	93.793	81.848(3)
γ [°]	68.483(3)	90	90	90	90	88.600(3)
V [Å^{-3}]	2263.67(12)	4999.1(5)	2123.50(13)	4424.6(2)	1044.5(11)	1285.51(8)
Z	2	8	4	4	2	2
ρ_{calcd} [g cm^{-3}]	1.525	1.455	1.472	1.518	1.496	1.461
λ [Å]	0.71073	0.71073	0.71073	0.71073	0.71073	0.71073
T [K]	180(2)	180(2)	180(2)	180(2)	180(2)	180(2)
$\mu(Mo_{K\alpha})$ [mm^{-1}]	1.017	0.925	1.074	1.039	1.092	0.905
R[a] obsd, all	0.0324, 0.0415	0.0423, 0.0947	0.0344, 0.0466	0.0413, 0.0477	0.0223, 0.0234	0.0352, 0.0373
Rw[b] obsd, all	0.0869, 0.0899	0.0972, 0.1256	0.0752, 0.0791	0.0941, 0.0978	0.0552, 0.0618	0.0892, 0.0907

[a] $R = \Sigma||F_o| - |F_c||/\Sigma|F_o|$. [b] $wR2 = [\Sigma w(|F_o^2| - |F_c^2|)^2/\Sigma w|F_o^2|^2]^{1/2}$.

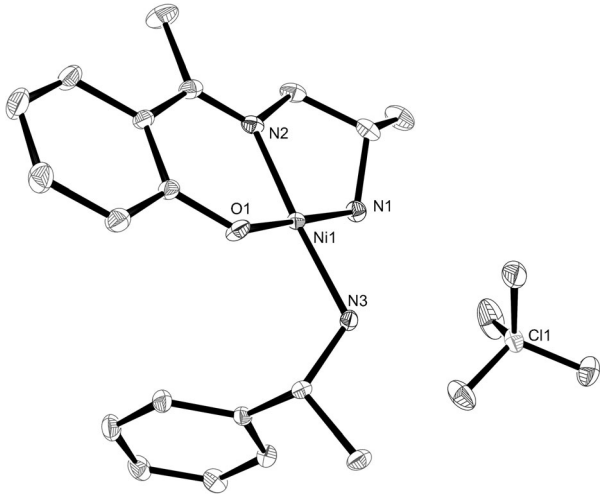

Figure 2. Plot of complex **7** with ellipsoids drawn at 30% probability and partial atom numbering. Hydrogen atoms have been omitted for clarity. Selected bond lengths [Å] and angles [°]: Ni1–O1 1.8149(19), Ni1–N1 1.894(2), Ni1–N2 1.869(2), Ni1–N3 1.940(2); O1-Ni1-N2 94.57(7), O1-Ni1-N3 87.47(7), N1-Ni1-N2 86.47(8), N1-Ni1-N3 91.36(8), O1-Ni1-N1 177.10(8), N2-Ni1-N3 176.57(8).

a chiral space group for **5**. Indeed, the two diastereoisomers $(S)_{ligand}$-$(R)_{amine}$ and $(R)_{ligand}$-$(R)_{amine}$ that coexist in complex **5** are chiral. Use of pure (*S*)-1,2-diaminopropane (**7**) yields a unique stereoisomer $(S)_{ligand}$-$(R)_{amine}$. The methyl substituent of the diamino chain is remote from the hydroxyacetophenone moiety, so that the remote (*R*) geometrical isomer alone is present in complexes **5** and **7**, as previously observed for complexes involving ligands derived from 1,2-diaminopropane.[40] The methyl group adopts a pseudo-equatorial orientation in each case, inducing a δ or λ *gauche* conformation of the five-membered ring formed by the diamine moiety chelating the nickel ion in the $(S)_{ligand}$-$(R)_{amine}$ and $(R)_{ligand}$-$(R)_{amine}$ molecules, respectively. It is noteworthy that the phenyl substituent of monodentate (*R*)-1-phenylethylamine is oriented in a plane parallel to the nickel N_3O coordination plane in complex **5** but lies in a perpendicular plane for complex **7**. This induces a different arrangement of the $(S)_{ligand}$-$(R)_{amine}$ isomers in complexes **5** and **7**. Although similar $NH_{2amine}\cdots OClO\cdots H_2N_{ligand}$ hydrogen bonds are present in both cases, the molecules are stacked in complex **7**, separated by 5.769(6) Å, while they have an helical arrangement in complex **5**, with an helix pitch of 7.972(7) Å involving two molecules per pitch, thus yielding two stacks of molecules rotated by 180°. The hydrogen bonds are limited to simple $NH_{2amine}\cdots OClO_3$ bonds in the $(R)_{ligand}$-$(R)_{amine}$ isomers, and these molecules are inserted in between the $(S)_{ligand}$-$(R)_{amine}$ isomers through CH···π stacking contacts.

The structure determination of $[\{L^1Ni(2,2'\text{-bipy})\}_2](ClO_4)_2$ (**2**) (Figure 3) confirmed that we have isolated a dinickel complex with six-coordinate Ni ions instead of the expected pentanuclear Ni complex. The two Ni ions are chelated by a tridentate ligand and a 2,2′-bipyridine ligand, and the deprotonated phenoxo oxygen atoms of the tridentate ligands bridge the two Ni ions. This hexacoordination is best described as a distorted octahedron, and the program SHAPE gave shape measure parameters S_{Oh} of 1.57 and 1.48 for Ni1 and Ni2, respectively.[41] The equatorial plane involves the tridentate ligand and one nitrogen atom of 2,2′-bipy, and the apical positions are occupied by the second nitrogen atom of 2,2′-bipy and the phenoxo oxygen atom of the neighboring tridentate ligand. The equatorial Ni–O bonds are shorter (2.020(1) and 2.025(1) Å) than the axial ones (2.167(1) and 2.118(1) Å). The Ni–N bonds involving primary amine nitrogen atoms (N3, N7) are longer (2.074(2), 2.085(2) Å) than the $Ni-N_{imine}$ bonds (N4, N8; 2.040(2), 2.045(2) Å) but they are comparable to the equatorial $Ni-N_{bipy}$ bonds (2.096(2), 2.080(2) Å). Surprisingly, the axial $Ni-N_{bipy}$ bonds are not significantly longer than the equatorial ones (2.099(2), 2.106(2) Å). The central four-atom Ni-O_2-Ni core of the molecule is characterized by Ni-O-Ni angles of 100.55(5) and 102.37(5)°. There are no hydrogen bonds between neighboring NiNi dicationic entities. These large intermolec-

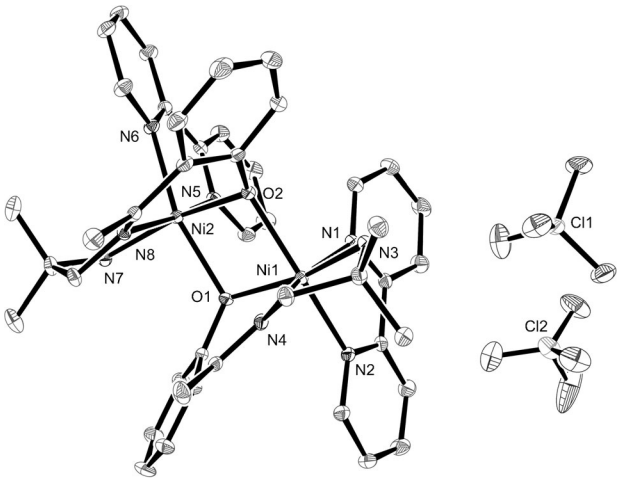

Figure 3. Plot of complex **2** with ellipsoids drawn at 30% probability and partial atom numbering. Hydrogen atoms have been omitted for clarity. Selected bond lengths [Å] and angles [°]: Ni1–O1 2.020(1), Ni1–O2 2.167(1), Ni1–N1 2.096(2), Ni1–N2 2.099(2), Ni1–N3 2.074(2), Ni1–N4 2.040(2), Ni2–O2 2.025(1), Ni2–O1 2.118(1), Ni2–N5 2.080(2), Ni2–N6 2.106(2), Ni2–N7 2.085(2), Ni2–N8 2.045(2); O1-Ni1-O2 77.97(5), N1-Ni1-N2 77.51(6), N2-Ni1-O2 163.26(6), N1-Ni1-N4 171.23(6), O1-Ni1-N3 164.18(6), Ni1-O1-Ni2 102.37(5), Ni1-O2-Ni2 100.55(5), O1-Ni2-O2 79.00(5), N5-Ni2-N6 77.36(6), N6-Ni2-O1 163.26(6), N5-Ni2-N8 171.26(6), O2-Ni2-N7 165.80(6).

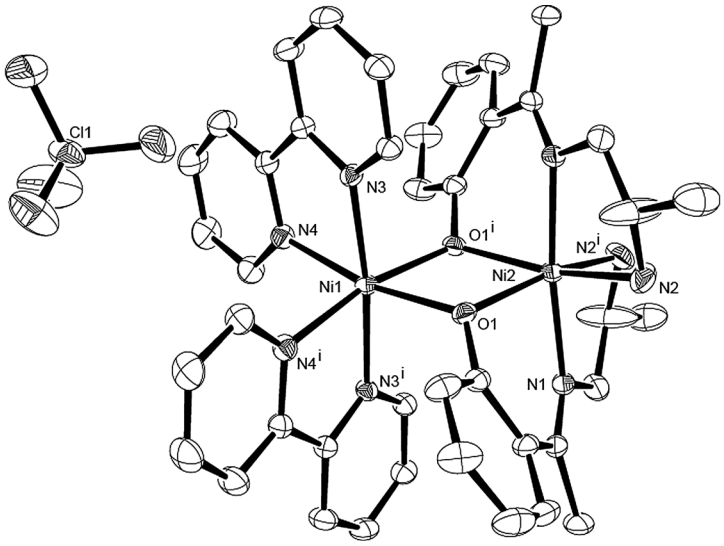

Figure 4. Plot of complex **6** with ellipsoids drawn at 30% probability and partial atom numbering. Hydrogen atoms have been omitted for clarity. Selected bond lengths [Å] and angles [°]: Ni1–O1 2.063(2), Ni1–O1^{i} 2.063(2), Ni1–N3 2.071(2), Ni1–N4 2.069(2), Ni1–N3^{i} 2.071(2), Ni1–N4^{i} 2.069(2), Ni2–O1 2.063(2), Ni2–O1^{i} 2.063(2), Ni2–N1 2.043(2), Ni2–N2 2.108(3), Ni2–N1 2.043(2), Ni2–N2 2.108(3); O1-Ni1-O1^{i} 78.36(11), N3-Ni1-N4 78.29(9), N3^{i}-Ni1-N4^{i} 78.29(9), N4-Ni1-O1 168.70(8), N4^{i}-Ni1-O1^{i} 168.70(8), N3-Ni1-N3^{i} 173.28(12), Ni1-O1-Ni2 101.63(8), N1-Ni2-N1^{i}-173.46(13), N2^{i}-Ni2-O1 163.04(9), N2-Ni2-O1^{i} 163.04(9).

ular distances suggest that the only active magnetic interaction involves the two nickel ions. Furthermore, helicity is introduced by coordination of a tridentate and a bidentate ligands around the nickel ion. Figure 3 shows that the two Ni ions of complex **2** have the same Λ helicity and that the five-membered nonplanar ring involving the diamino chain of the tridentate ligand is in a δ *gauche* conformation. Complex **2** crystallizes in centrosymmetric space group $P\bar{1}$ with $Z=2$, which means that the second molecule corresponds to the ΔλΔλ conformer.

In view of the structure of complex **2**, complex **6**, which results from reaction of complex **5** with 2,2′-bipyridine, is expected to be a dinickel complex. Although we indeed have a dinuclear complex, the structure determination shows scrambling of the two ligands (Figure 4). One Ni ion is surrounded by two trinuclear ligands, while the coordination sphere of the other involves two 2,2′-bipyridine ligands and two oxygen atoms of the trinuclear ligands. Furthermore, these two deprotonated phenoxo oxygen atoms bridge the two Ni ions. Contrary to complex **2**, the central Ni-O_2-Ni core is more symmetric, with equal Ni–O bond lengths (2.063(2) Å). Nevertheless the Ni-O-Ni angle of 101.6(1)° corresponds to the mean value observed in **2**. There is a larger difference between the Ni–N_{imine} bond lengths (2.043(2) Å), which are in *trans* position, and the Ni–N primary amine bonds (2.103(3) Å) than in complex **2**, and there is no difference between the axial and equatorial Ni–N_{bipy} bond lengths (2.069(2), 2.071(2)Å). In Figure 4, the Ni1 ion has Λ helicity, while Ni2 is chelated by two tridentate ligands having their asymmetric carbon atom in the *S* configuration. The other conformer with Ni1 Δ helicity and two *R* carbon atoms around Ni2 is also present in the crystal, due to the centrosymmetric *C*2/*c* space group. These dinuclear molecules are well isolated from each other, and hydrogen bonding is limited to intramolecular NH_2(amine)···$OClO_3$ bonds. The SHAPE program indicates that the octahedron is less deformed for Ni1 ($S_{Oh}=1.11$) than for Ni2 ($S_{Oh}=1.58$).[41]

Replacement of 2,2′-bipyridine by the more crowded 6,6′-dimethyl-2,2′-bipyridine in the reaction with complex **1** yields complex **3**. The structure determination of [L^1Ni(6,6′-diMe-2,2′-bipy)]ClO_4 (**3**) confirmed that the Ni ion is pentacoordinate and that it crystallizes in centrosymmetric space group *C*2/*c*. The SHAPE program indicates that the Ni coordination sphere is better described as a square pyramid ($S_{Py}=1.49$) than a vacant octahedron ($S_{VOC}=1.81$)[42] with the tridentate ligand and a nitrogen atom of the dimethyl-substituted bipyridine in the basal plane, while the other nitrogen atom is in the apical position. The Δδ and Λλ diastereomers are present in the crystal; the Λλ form is shown in Figure 5. The Ni–N and Ni–O bonds are slightly shorter than in complex **2** (see caption to Figure 5). These molecules are well isolated from each other, for there is no intramolecular or intermolecular hydrogen bond.

To simplify the structural data, complex **8** was prepared by using enantiomerically pure complex **7**. This complex crystallizes in the noncentrosymmetric space group *P*1 (Figure 6). The main difference to complex **3** comes from introduction of a chiral center in the tridentate ligand, which gives Δ and Λ stereomers that do not become superimposa-

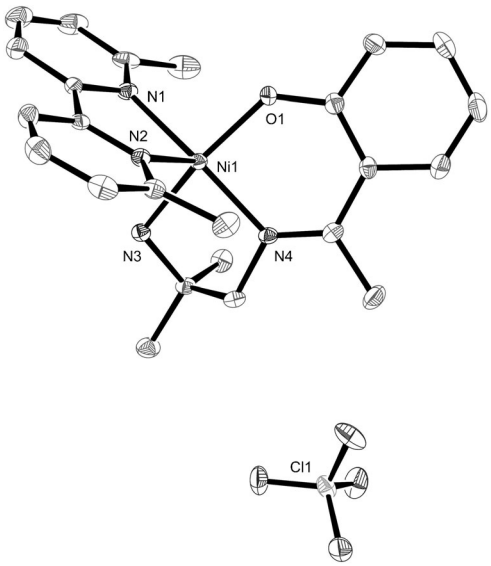

Figure 5. Plot of complex **3** with ellipsoids drawn at 30% probability and with partial atom numbering. Hydrogen atoms have been omitted for clarity. Selected bond lengths [Å] and angles [°]: Ni1–O1 1.906(2), Ni1–N1 2.065(3), Ni1–N2 2.058(3), Ni1–N3 2.091(3), Ni1–N4 2.022(3); 166.3(1).

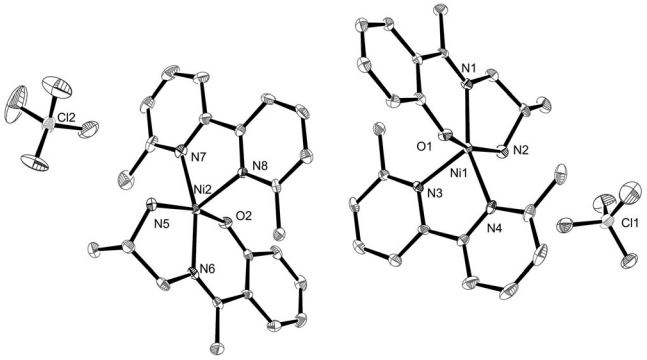

Figure 6. Plot of complex **8** with ellipsoids drawn at 30% probability and with partial atom numbering. Hydrogen atoms have been omitted for clarity. Selected bond lengths [Å] and angles [°]: Ni1–O1 1.957(3), Ni1–N1 2.009(4), Ni1–N2 2.065(4), Ni1–N3 2.048(4), Ni1–N4 2.044(4), Ni2–O2 1.958(3), Ni2–N5 2.071(4), Ni2–N6 2.017(4), Ni2–N7 2.040(4), Ni2–N8 2.044(4); O1-Ni1-N2 166.4(2), O1-Ni1-N3 98.1(2), N1-Ni1-N3 119.8(2), N2-Ni1-N3 95.6(2), N3-Ni1-N4 81.4(2), N1-Ni1-N4 158.7(2), O2-Ni2-N5 167.0(2), O2-Ni2-N8 98.7(2), N5-Ni2-N8 94.2(2), N6-Ni2-N7 161.9(2), N6-Ni2-N8 117.7(2), N7-Ni2-N8 80.3(2)°.

ble when the conformation of the nonplanar five-membered ring is changed. The Δ stereomer has a δ *gauche* conformation, with the methyl group of 1,2-diaminopropane in an axial position, while the Λ stereomer has a λ *gauche* conformation and the methyl group in equatorial position. The Ni–N and Ni–O bonds are slightly shorter than in complex **3**, except for the Ni–O bonds that are longer in the two stereomers (1.957(3) and 1.958(3) vs. 1.906(2) Å). The SHAPE program confirms that the Λ stereomer can be equally considered as a distorted vacant octahedron or a distorted square pyramid ($S_{VOC}=1.95$, $S_{Py}=1.96$) while the distorted square pyramid is slightly favored in the Δ form ($S_{Py}=1.88$, $S_{VOC}=2.12$).[42] Very similar hydrogen NH_2(amine)···$OClO_3$ and NH_2(amine)···OHMe bonds link the cationic [L^1Ni(6,6′-diMe-2,2′-bipy)] entities to the perchlorate anion and to the MeOH molecule of crystallization in the two stereomers. A supplementary MeOH···OC hydrogen bond, characterized by a H···OC distance of 2.798(5) Å, links the Λ molecules, which stack with an Ni···Ni distance of 8.197(6) Å. Such a bond is not present in the Δ stereomer, in which the H···OC distance is 3.073(5) Å. Nevertheless, weak contacts again induce stacking of these molecules with a similar Ni···Ni spacing of 8.197(6) Å.

Magnetic properties: *Experimental studies*: According to the structural studies, square-planar nickel complexes **1**, **5**, and **7** are diamagnetic with low-spin Ni ions, so only complexes **2**, **3**, **6**, and **8** were studied. The magnetic susceptibilities of these four Ni complexes were measured in the temperature range 2–300 K under an applied magnetic field of 0.1 T. The thermal variation of $\chi_M T$ for complex **2** is displayed in Figure 7, where χ_M is the molar magnetic susceptibility of

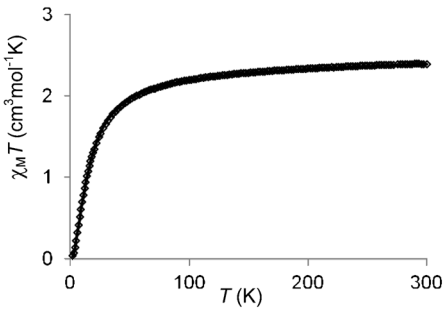

Figure 7. Temperature dependence of $\chi_M T$ for **2** from 300 to 2 K. The solid line corresponds to the best fit ($J=-8.8\ cm^{-1}$, $g=2.17$).

the dinuclear species corrected for the diamagnetism of the ligands. The $\chi_M T$ value of 2.39 $cm^3 mol^{-1} K$ at 300 K slightly decreases down to 50 K (1.95 $cm^3 mol^{-1} K$) before abruptly decreasing to 0.03 $cm^3 mol^{-1} K$ at 2 K. The room-temperature $\chi_M T$ value corresponds to what is expected for two isolated nickel ions with a g parameter slightly larger than 2. The magnetic susceptibility was computed by exact calculation of the energy levels through diagonalization of the full energy matrix with a Hamiltonian including only isotropic exchange: $H=-J_{NiNi}(S_{Ni1}\cdot S_{Ni2})+\Sigma_{i,j}\ g_i\beta H_j S_{ij}$ with i=Ni and $j=x,y,z$. The best fit (solid line in Figure 7) yields the following data: $J=-8.8\ cm^{-1}$ and $g=2.17$ with an R factor of $R=\Sigma[(\chi_M T)^{obsd}-(\chi_M T)^{calcd}]^2/\Sigma(\chi_M T)^{obsd}]^2=4.0\times10^{-5}$. To check the validity of these results, the Magpack program was used to fit the experimental magnetization curve at low temperature. However, as shown in Figure S1 of the Supporting Information, the low-field regime of the magnetization curve is not well accounted for by only using isotropic interactions in the spin Hamiltonian (solid line). Since in complex **2**, all kinds of anisotropic interactions are symmetry-allowed (no

symmetry element is observed in the molecular unit), all of these interactions are susceptible to being of comparable magnitude, and that this complex belongs to the weak-exchange limit, the introduction of anisotropic interactions in the model Hamiltonian is expected to be problematic (as stated in the Introduction). Surprisingly, the introduction of only a local anisotropy term, namely, $H=-J_{NiNi}(S_{Ni1}\cdot S_{Ni2})+D_{Ni}(S^2_{z,Ni1}+S^2_{z,Ni2})$ already leads to satisfactory fitting of the low-field regime (see Figure S2 of the Supporting Information). However, due to the crudeness of such modeling, which neglects the mismatch between the principal axes of the local anisotropies and the anisotropic interactions, the extracted value of D_{Ni} is not considered to be meaningful at this stage. A more detailed study of the importance of all effective interactions would be required, but necessitates further experimental techniques more sensitive to the wave function of the lowest-lying spin–orbit states, and/or highly demanding ab initio calculations. Such a study in itself would deserve a full paper, and is outside the scope of the present work dealing mainly with the synthesis of new compounds that are of interest for molecular magnetism.

Similar behavior is observed for the other dinuclear complex **6**, except that the interaction parameter is weaker: $J=-2.2\ cm^{-1}$, $g=2.18$ (Figure 8). As in complex **2**, the magnetization curve at 2 K cannot be fitted by these parameters, and an approximate fit again necessitates introduction of a local D term.

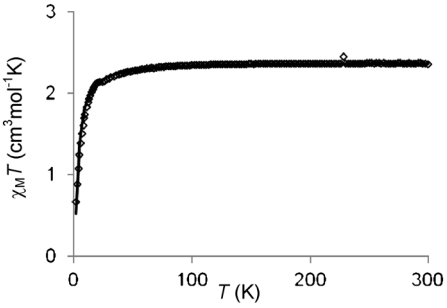

Figure 8. Temperature dependence of $\chi_M T$ for **6** from 300 to 2 K. The solid line corresponds to the best fit ($J=-2.2\ cm^{-1}$, $g=2.18$).

In complexes **3** and **8** the nickel ions are the only magnetically active metal centers, and the structure determinations have shown that these molecules are well isolated from each other. Their magnetic behaviors are quite similar. The $\chi_M T$ value of complex **3** is $1.15\ cm^3 mol^{-1} K$ at 300 K, remains constant down to 30 K ($1.13\ cm^3 mol^{-1} K$), and then decreases to $0.20\ cm^3 mol^{-1} K$ at 2 K (Figure 9). The room-temperature $\chi_M T$ value corresponds to the value expected for an isolated nickel ion with $g=2.17$. The magnetic susceptibility was computed by exact calculation of the energy levels through diagonalization of the full energy matrix with an Hamiltonian introducing axial and rhombic zero-field splitting terms. The best fit (solid line in Figure 9) yields $D_{Ni}=15.9\ cm^{-1}$, $E=0$, $g=2.17$ with $R=6.0\times10^{-5}$, values that

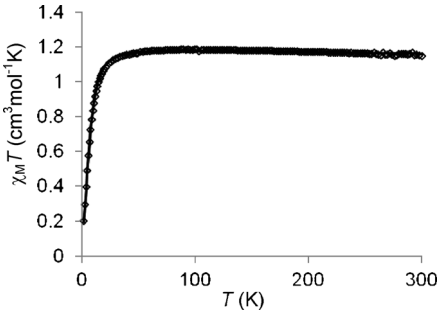

Figure 9. Temperature dependence of $\chi_M T$ product **3** from 300 to 2 K. The solid line corresponds to the best fit ($D_{Ni}=15.9\ cm^{-1}$, $g=2.17$).

nicely fit the experimental magnetization curve at 2 K (Figure S3 of the Supporting Information). The same treatment applied to complex **8** (Figures S4 and S5 of the Supporting Information) gives $D_{Ni}=16.7\ cm^{-1}$, $g=2.18$. It appears that introduction of a E term gives a slightly better fit of the experimental magnetization ($E=0.6\ cm^{-1}$).

Ab initio calculations: Ab initio calculations of the ZFS parameters were performed for mononuclear complexes **3** and **8**, and the results are presented in Table 2. The large anisotropy of complex **3** is confirmed by SI calculations per-

Table 2. Computed ZFS parameters for complexes **3** and **8**. Both stereomers of complex **8** are considered. The diagonal elements of the SI matrix are the energies obtained at the CASSCF or NEVPT2 levels.

Complex	Method	$D\ [cm^{-1}]$	$E\ [cm^{-1}]$	$E/\lvert D\rvert$
3	CASSCF	+32.5	9.7	0.30
	NEVPT2	+21.9	7.0	0.32
Δ-**8**	CASSCF	+28.2	1.8	0.06
	NEVPT2	+18.3	1.8	0.10
Λ-**8**	CASSCF	+29.6	0.9	0.03
	NEVPT2	+19.2	1.2	0.06

formed with either the CASSCF and NEVPT2 energies on the diagonal elements of the interaction matrix, in agreement with a nearly SPY geometry around the Ni ion. However, since the $E/|D|$ ratio is found to be close to 1/3, the sign of the axial D parameter cannot be confirmed by the calculations. Since no satisfactory fit was obtained with negative D parameters for the magnetic susceptibility and magnetization curves, it is concluded that such a situation is probably due to overestimation of the rhombic anisotropy in the calculations. Previous works already showed that computed ZFS parameters are usually larger than the experimentally determined ones,[9–10] and this was explained by uncertainties in either or both the experimental and theoretical approaches. These new results tend to show that our theoretical calculations overestimate the rhombic parameters, but further studies would be required to confirm such a statement.

Both Δ and Λ stereomers of complex **8** were considered (see Table 2). Since the difference between the two struc-

tures is located far from the magnetic center, no significant difference is expected between the ZFS of the two stereomers. Such hypothesis is undoubtly confirmed by our calculations, which justifies that the ZFS of the complex can be experimentally determined as a single entity. The axial D parameter was found to be large and positive, as expected for a nearly SPY structure. The inclusion of dynamic correlation affects the ZFS and confirms a large positive D parameter, in agreement with experiment.

Even if the D sign in complex **3** could not be determined only from theory in this work, we conclude that our ab initio calculations confirm that we have synthesized mononuclear complexes with large single ion anisotropies.

Discussion

The structural determinations confirm that the experimental process described here is able to give new tridentate ligands. Due to the possibility of hydrolysis, it is not easy to isolate such ligands, but coordination chemistry simplifies the problem. Indeed, once linked to a metal ion, they are quite stable, as demonstrated by the structural determinations of complexes **5** and **7**. These structural data also show that the reactive amino group is always the primary amine remote from the substituted alkyl chain. The use of an enantiomerically pure form of the monodentate amine, which is coordinated to the fourth equatorial position of the Ni ion, is responsible for the observation of a chiral space group in complexes **5** and **7**, while the pure stereoisomer $(S)_{ligand}$-$(R)_{amine}$ was characterized when pure (*S*)-diaminopropane was used (complex **7**), and two diastereoisomers $(S)_{ligand}$-$(R)_{amine}$ and $(R)_{ligand}$-$(R)_{amine}$ coexist in complex **5**. The following step, which consists of replacing the monodentate ligand by the bidentate 2,2′-bipyridine, is favored by the chelate effect. Although this reaction works nicely, it does not necessarily furnish the expected pentacoordinate Ni complex, as demonstrated by the structural determination of complexes **2** and **6**, in which the phenoxo oxygen atom of a pentacoordinate Ni unit is able to link to the Ni ion of a neighboring unit, thus yielding a dinuclear complex with hexacoordinate Ni ions. Such a situation can be avoided if the Ni units are far enough from each other. Thus replacement of 2,2′-bipyridine by the more crowded 6,6′-dimethyl-2,2′-bipyridine favors preparation of pentacoordinate Ni complexes **3** and **8**. Lengthening of the Ni–O and Ni–N bonds is observed on going from the square-planar Ni environment (**5**, **7**) to square-pyramidal (**3**, **8**) and, to a lesser extent, to octahedral Ni coordination (**2**, **6**).

Observation of an antiferromagnetic Ni–Ni interaction agrees with literature data showing that antiferromagnetic behavior is associated with Ni-O-Ni angles around 100°.[43] In complex **2**, the Ni-O_2-Ni core of the molecule is characterized by Ni-O-Ni angles of 102.37(5) and 100.55(5)° and an interaction parameter of $-8.8\ cm^{-1}$. The geometry of the coordination octahedron for each Ni ion in **2** corresponds to a slightly elongated bipyramid, with O2, N2 and O1, N6 in axial position for the Ni1 and Ni2 ions, respectively. A recent reinvestigation of the axial zero-field splitting[44] allows a tetragonality parameter D_{str} to determined if the metal–ligand bond lengths are known and eventually an estimation of a D_{mag} term defining the Ni magnetic anisotropy. Applying this to complex **2** gives D_{str} terms of the Ni1 and Ni2 centers of 11.12 and 9.12, which give D_{mag} values of 7.44 and $6.18\ cm^{-1}$, respectively. This analysis confirms the presence of single-ion anisotropies in this complex that cannot be determined in a straightforward way from experiment due to the mismatch between the principal axes of the local anisotropies and the presence of intersite anisotropies. A similar behavior is obtained in complex **6**, with a smaller antiferromagnetic coupling between the magnetic sites. Although we could not obtain crystals of complex **4** suitable for XRD analysis, magnetic data are informative. In the solid state, complex **4** is diamagnetic. Its orange color agrees with a square-planar Ni environment and monodentate acetate coordination. Dissolution in water gives a colorless solution, in agreement with an evolution toward a high-spin octahedral species. This would imply that the acetate anion is coordinated to the Ni ion by only one oxygen atom in the solid state, while hexacoordination of the Ni ion is completed by water molecules and perhaps acetate chelation or dimerization.[45]

Conclusion

A synthetic stepwise process able to give mononuclear nickel complexes with a pentacoordinate environment has been described. It is based on the use of tridentate ligands, known as half-units, resulting from monocondensation of a diamine with a ketone group. One example is straightforward because the steric hindrance of one primary amino group impedes the reaction with the ketone. The second example gives a genuine tridentate ligand that can be isolated as a nickel complex and not as a pure organic ligand. Whatever the tridentate ligand, it is first coordinated to a nickel ion, while a monodentate nitrogen base occupies the fourth position of the resulting square-planar and diamagnetic nickel complex. The next step consists of introducing a bidentate ligand such as 2,2′-bipyridine or 6,6′-dimethyl-2,2′-bipyridine. Structure determinations showed that the process does not work with 2,2′-bipyridine. Indeed dinuclear complexes are then characterized, and hexacoordination of the nickel ions comes from the bridging function of the phenoxo oxygen atoms of the tridentate ligands. Surprisingly, two different dinuclear complexes were observed. Although they both have a double phenoxo bridge, each nickel ion is surrounded by a tridentate and a bidentate ligands in one case while a ligand scrambling leads to a dinuclear unit in which the coordination sphere of one nickel ion contains the two tridentate ligands while the second sphere involves the two bidentate ligands and the two bridging phenoxo oxygen atoms. These changes in coordination environment result in different antiferromagnetic interactions of −8.8 and

$-2.2\ cm^{-1}$, respectively. On the contrary, use of the sterically hindered 6,6′-dimethyl-2,2′-bipyridine results eventually in the desired pentacoordinate nickel complexes. The assembly process of a tridentate and a bidentate ligand around a nickel ion is original and not used in previous works.

The ZFS parameters of the two mononuclear pentacoordinate nickel complexes were studied by means of magnetic data and state-of-the-art ab initio calculations. As in previous studies dealing with nickel complexes, good agreement between the computed and experimental ZFS parameters was obtained. As a consequence, the calculations confirm the large magnitudes of the single-ion anisotropies of the complexes presented here. Such a result is in agreement with the geometry of the first coordination spheres around the Ni ions, which show a nearly SPY structure in both complexes. However, for one complex, the calculated parameters led to an $E/|D|$ ratio close to 1/3, which prohibits determination of the sign of D from the calculations. Such a result is attributed here to overestimation of the rhombic anisotropy in the ab initio calculations, which would deserve further theoretical studies.

Acknowledgements

This work was supported by the Spanish Ministry of Science and Innovation (project CTQ2008-06644-C02-01), the Generalitat de Catalunya (project 2009SGR462 and Xarxa d′R+D+I en Química Teòrica I Computacional, XRQTC), the French Research Agency (Agence Nationale de la Recherche, reference ANR-09-BLAN-0054-01 and project TEMAMA ANR-09-BLAN-0195-01).

[1] J. N. Rebilly, G. Charron, E. Rivière, R. Guillot, A. L. Barra, M. Duran Serrano, J. van Slageren, T. Mallah, *Chem. Eur. J.* **2008**, *14*, 1169–1177.
[2] M. R. Pederson, S. N. Khanna, *Phys. Rev. B* **1999**, *60*, 9566–9572.
[3] M. Atanasov, C. A. Daul, C. Rauzy, *Chem. Phys. Lett.* **2003**, *367*, 737–746.
[4] A. Borel, L. Helm, C. A. Daul, *Chem. Phys. Lett.* **2004**, *383*, 584–591.
[5] F. Aquino, J. H. Rodriguez, *J. Chem. Phys.* **2005**, *123*, 204902.
[6] F. Neese, *J. Am. Chem. Soc.* **2006**, *128*, 10213–10222.
[7] F. Neese, *J. Chem. Phys.* **2007**, *127*, 164112.
[8] D. Ganyushin, F. Neese, *J. Chem. Phys.* **2006**, *125*, 024103.
[9] R. Maurice, L. Vendier, J. P. Costes, *Inorg. Chem.* **2011**, *50*, 11075–11081.
[10] R. Maurice, R. Bastardis, C. de Graaf, N. Suaud, T. Mallah, N. Guihéry, *J. Chem. Theory Comput.* **2009**, *5*, 2977–2984.
[11] R. Maurice, C. de Graaf, N. Guihéry, *J. Chem. Phys.* **2010**, *133*, 084307.
[12] R. Maurice, A. M. Pradipto, N. Guihéry, R. Broer, C. de Graaf, *J. Chem. Theory Comput.* **2010**, *6*, 3092–3101.
[13] R. Maurice, K. Sivalingam, D. Ganyushin, N. Guihéry, C. de Graaf, F. Neese, *Inorg. Chem.* **2011**, *50*, 6229–6236.
[14] R. Maurice, N. Guihéry, R. Bastardis, C. de Graaf, *J. Chem. Theory Comput.* **2010**, *6*, 55–65.
[15] E. Liviotti, S. Carretta, G. Amoretti, *J. Chem. Phys.* **2002**, *117*, 3361–3368.
[16] S. Carretta, E. Liviotti, N. Magnani, P. Santini, G. Amoretti, *Phys. Rev. Lett.* **2004**, *92*, 207205.
[17] R. Maurice, C. de Graaf, N. Guihéry, *Phys. Rev. B* **2010**, *81*, 214427.
[18] F. A. Cotton, G. Wilkinson, *Advanced Inorganic Chemistry*, 5th ed, Wiley, New York, **1988**.
[19] D. L. Kepert, *Inorganic Stereochemistry, Inorganic Chemistry Concepts, Vol. 6*, Springer, Berlin, **1982**.
[20] J. P. Costes, *Bull. Soc. Chim. Fr.* **1986**, 78–82; J. P. Costes, F. Dahan, M. B. Fernandez Fernandez, M. I. Fernandez Garcia, A. M. Garcia Deibe, J. Sanmartin, *Inorg. Chim. Acta* **1998**, *274*, 73–81.
[21] J. P. Costes, M. I. Fernandez Garcia, *Inorg. Chim. Acta* **1995**, *237*, 57–63.
[22] P. Pascal, *Ann. Chim. Phys.* **1910**, *19*, 5–70.
[23] A. K. Boudalis, J. M. Clemente-Juan, F. Dahan, J. P. Tuchagues, *Inorg. Chem.* **2004**, *43*, 1574–1586.
[24] J. J. Borrás-Almenar, J. M. Clemente-Juan, E. Coronado, B. S. Tsukerblat, *Inorg. Chem.* **1999**, *38*, 6081–6088; J. J. Borrás-Almenar, J. M. Clemente-Juan, E. Coronado, B. S. Tsukerblat, *J. Comput. Chem.* **2001**, *22*, 985–991.
[25] F. James, M. Roos, M. " *MINUIT Program*, a System for Function Minimization and Analysis of the Parameters Errors and Correlations"; *Comput. Phys. Commun.* **1975**, 10, 343–367.
[26] SIR92 - A program for crystal structure solution. A. Altomare, G. Cascarano, C. Giacovazzo, A. Guagliardi, *J. Appl. Crystallogr.* **1993**, *26*, 343–350.
[27] SHELX97 [includes SHELXS97, SHELXL97, CIFTAB] - Programs for Crystal Structure Analysis (Release 97–2). G. M. Sheldrick, Institüt für Anorganische Chemie der Universität, Tammanstrasse 4, 3400 Göttingen, Germany, **1998**.
[28] WINGX - 1.63 Integrated System of Windows Programs for the Solution, Refinement and Analysis of Single Crystal X-Ray Diffraction Data. L. Farrugia, *J. Appl. Crystallogr.* **1999**, *32*, 837–838.
[29] *International Tables for X-ray Crystallography, Vol. IV*, Kynoch press, Birmingham, England, **1974**.
[30] ORTEP32 for Windows: L. Farrugia, *J. Appl. Crystallogr.* **1997**, *30*, 565–568.
[31] F. Neese, ORCA-An ab initio, density functional and semiempirical program package v. 2.8, University of Bonn, Bonn, Germany.
[32] C. Angeli, R. Cimiraglia, J.-P. Malrieu, *Chem. Phys. Lett.* **2001**, *350*, 297–305.
[33] C. Angeli, R. Cimiraglia, J.-P. Malrieu, *J. Chem. Phys.* **2002**, *117*, 9138–9153.
[34] C. Angeli, M. Pastore, R. Cimiraglia, *Theor. Chem. Acc.* **2007**, *117*, 743–754.
[35] F. Neese, *J. Chem. Phys.* **2005**, *122*, 034107.
[36] B. A. Hess, C. M. Marian, U. Wahlgren, O. Gropen, *Chem. Phys. Lett.* **1996**, *251*, 365–371.
[37] C. Bloch, *Nucl. Phys.* **1958**, *6*, 329–347.
[38] J. Des Cloizeaux, *Nucl. Phys.* **1960**, *20*, 321–346.
[39] F. Weigend, R. Ahlrichs, *Phys. Chem. Chem. Phys.* **2005**, *7*, 3297–3305.
[40] J. P. Costes, F. Dahan, J. M. Dominguez Vera, J. P. Laurent, J. Ruiz, J. Sotiropoulos, *Inorg. Chem.* **1994**, *33*, 3908–3913.
[41] S. Alvarez, D. Avnir, M. Llunell, M. Pinsky, *New J. Chem.* **2002**, *26*, 996–1009.
[42] S. Alvarez, M. Llunell, *J. Chem. Soc. Dalton Trans.* **2000**, 3288–3303.
[43] L. Ballester, E. Coronado, A. Gutiérrez, A. Monge, M. F. Perpinan, E. Pinilla, T. Rico, *Inorg. Chem.* **1992**, *31*, 2053–2056; W. L. Glandfelter, M. W. Lynch, W. P. Schaefer, D. N. Hendrickson, H. B. Gray, *Inorg. Chem.* **1981**, *20*, 2390–2397; M. A. Halcrow, J. S. Sun, J. C. Huffman, G. Christou, *Inorg. Chem.* **1995**, *34*, 4167–4177.
[44] J. Titis, R. Boca, *Inorg. Chem.* **2010**, *49*, 3971–3973.
[45] J. P. Costes, F. Dahan, J. P. Laurent, *Inorg. Chem.* **1985**, *24*, 1018–1022.

Received: November 18, 2011
Published online: February 22, 2012

